Shear strength of steel reinforced concrete (SRC) columns

Autor(en): **Minami, Koichi / Wakabayashi, Minoru**

Objekttyp: **Article**

Zeitschrift: **IABSE reports of the working commissions = Rapports des commissions de travail AIPC = IVBH Berichte der Arbeitskommissionen**

Band (Jahr): **16 (1974)**

PDF erstellt am: **25.05.2024**

Persistenter Link: https://doi.org/10.5169/seals-15744

Shear Strength of Steel Reinforced Concrete (SRC) Columns

Résistance au cisaillement des colonnes en béton armé

Schubfestigkeit von Stahlbetonstützen

Koichi MINAMI
Lecturer
Osaka Institute of Technology
Osaka, Japan

Minoru WAKABAYASHI
Professor
Disaster Prevention Research Institute
Kyoto University
Kyoto, Japan

1. INTRODUCTION

Composite steel section and reinforced concrete structure which is called SRC structure has been widely used for buildings with more than 7 stories in Japan since these structures gave an excellent performance against The Kanto Earthquake of 1923. The first edition of the design specification for SRC system was published in 1958 by Architectural Institute of Japan and the revised edition was published in 1963. And now the third edition is being prepared in which the main part for revision is anticipated to be the design of columns under shear force. For this purpose a working group for the shear tests of SRC columns(Chairman is Dr. S. Takada) was formed in the SRC Subcommittee(Chairman is Dr. T. Naka) belonging to Architectural Institute of Japan. This paper presents an outline of the experiments conducted by the working group, and some results.

Very few experimental study on shear resistance of SRC columns had been conducted till recent years(1, 2). Recently some experimental works have been conducted by the authors(3), and the test program in the present paper is designed in reference to these recent works.

Forty two full scale SRC column specimens with full-web type, lattice and butten plate type open-web steel sections, and one ordinary reinforced concrete column specimen are tested under constant axial load and alternately repeated bending moment and shear. All specimens fail in shear. The shear capacities, failure modes, unloading characteristics in large deformation range, effect of cyclic loading on the shear resistance, and shapes of hysteresis curves are investigated.

2. TESTS

a. Test Plan: 3 types of the steel cross section are chosen for each specimen as shown in Fig. 1; full-web(F series), Lattice type open-web(L series) and butten plate type open-web(B series). The value of shear span ratio, h/D (h: column length, D: depth), is fixed to be 3 for all specimens except 3 specimens, for which h/D is selected to be 5 to investigate the effect of the shear span ratio. In Tables 1, 2 and 3, shown are the identification number for each specimen and the values of the experimental parameters. As the experimental parameters, selected for the specimens in F series are; flange thickness(t_f), web thickness(t_w), amount of main feinforcements(n, ϕ), spacing of web reinforcements(s), concrete strength(F_c), axial load ratio(N/N_o) and shear span ratio(h/D). N is the applied axial load, and N_o is the maximum compressive strength of the cross section computed by summing the contributions from each components; concrete, steel, and main reinforcing bars. For L series, inclination angle of lattice plate(θ), lattice plate thickness(t_l), spacing of web reinforcement and axial load ratio are selected, and ratio of spacing of butten plate to depth of steel section(p), butten plate thickness(t_b), spacing of web reinforcements and axial load ratio are selected for B series. In order to compare the shear failure, a specimen of ordinary reinforced concrete column (No. 43) is included in the test plan.

b. Material Properties: Details of reinforced concrete portion of the cross section, dimensions and arrangement for reinforcing bars, and shapes and dimensions of steel portion are shown in Figs. 2, 3 and 4, respectively. For the main reinforcements and web reinforcements, deformed bars SD35(guaranteed yield stress: 3.5ton/cm^2) and round bars SR24(2.4ton/cm^2) with diameter of 4.5 mm are used, respectively. The steel portion for each specimen is built up by welding, from SS41 steel plates(2.4ton/cm^2). The used concrete is a mixture of ordinary Portland cement, coarse aggregates(river gravel, maximum size less than 10mm) and fine aggregates(river sand maximum size less than 2.5mm).

c. Loading Apparatus: The loading apparatus and principle are shown in Figs. 5 and 6, respectively. Detail of this apparatus is omitted in this paper, since it was already presented at 5WCEE(4). Data detecting system for the relative displacement between the column top and bottom, δ, is shown in Fig. 7. The chord rotation angle R is given by δ/h.

d. Loading Program: Figures 8(a) and (b) show the loading programs employed in the test, in which the cyclic loading is controlled by the prescribed amplitude of the chord rotation angle, R.

e. Axial Load: Shown in Fig. 9 are the results of the investigation on the intensity of the axial load in columns of the first story of the actually constructed, regular shaped steel reinforced concrete buildings. The values of the axial load ratio, N/N_o, in the column of the first story scatter in the range from 0.1 to 0.4, and the mean value is about 0.2. Based on Fig. 9, the axial load ratios in the test are determined.

3. TEST RESULTS

a. Crack Observation: In all specimens except the reinforced concrete column, the diagonal tension crack appears at the angle R of ± 0.003rad., and the shear bond crack appears along the main reinforcement or the steel flange when the chord rotation angle, R, reaches to ± 0.005 to ± 0.01rad. In the process after the attainment of the maximum strength, the shear bond crack continues to grow to the whole length of the column, while the crack due to the diagonal tension stops to grow, as shown in Fig. 10.

The bare steel portions after the test are investigated by taking the concrete off. The local buckling of neither flange nor web plates is observed in F series, while the damage on the web of the open-web steel portion is quite severe, such as the fracture and buckling of lattice plates in L series, and the fracture of butten plates at the joint to the chord member in B series.

b. Hysteretic Characteristics: Some sample hysteretic relations between the applied shear force, Q, and the displacement, δ(or the chord rotation, R), obtained in the tests are shown in Figs. 11(a) to (c). Specimens in F series show stable, spindle-shaped hysteresis loops, and large energy absorption capacities. The maximum shear strength is attained under the loading controlled by R of $\pm$0.010 to $\pm$0.015rad and the rate of the strength reduction after that is slow. When R reaches to $\pm$0.03rad., the loop seems to converge to that of the bare steel portion. In case of specimens in L and B series, when R is $\pm$0.005rad. to $\pm$0.01rad., the maximum shear strength is attained, followed by the quick strength reduction, and the hysteresis loop is the reversed S-shaped. Particularly in B series, the energy absorption capacity is very small.

Figure 12 shows the strength reduction when the cyclic loading is applied on the specimen under a fixed value of the displacement amplitude. The strength reduction factor(the ratio of the maximum strength attained in each cycle of loading to the maximum strength in the first cycle under that amplitude) is taken for the ordinate, and the number of loading cycles is taken for the abscissa. Solid circles are the data in the positive loading, and open circles the negative loading. In general, the strength reduction factor converges to a certain value after 3 cycles of loading; about 80% in F series, about 70% in L series, and about 60% in B series.

c. Effects of Experimental Parameters: In Figs. 13(a) to (e), the sustained load and the chord rotation angle at the returning point in the first cycle of positive loading under each displacement amplitude are plotted in Q-R coordinates, with taking concrete strength, flange and web thicknesses, lattice and butten plate thicknesses, the amount of web reinforcement, and the axial load ratio as varying parameters. The shear strength increases with the increase of those parameters except the axial load ratio which seems not to affect much on the shear strength, as long as the present test results are concerned. It is interesting to note that in each of the figures straight lines with an nearly equal negative slope are obtained by connecting the data at the returning points after the attainment of the maximum shear strength.

4. DISCUSSIONS ON THE TEST RESULTS

For each specimen, the maximum shear strength $\tilde{Q}_{max}$(solid circle) in the whole history of loading, and the minimum shear strength $\tilde{Q}_{min}$(open circle) detected at the negative loading under R = $\pm$0.03rad., are plotted in Fig. 14, where $\tilde{Q}$ is equal to the sum of the applied shear force Q and NR/2 due to the secondary moment. Ratios of $\tilde{Q}_{max}$ and $\tilde{Q}_{min}$ to Q_{mo} are shown in Fig. 15, where Q_{mo} is computed from the maximum flexural strength of the cross section obtained by the method of superposition. The ratios of $\tilde{Q}_{max}/Q_{mo}$ are about 70% in F series, and about 50% in L and B series, and it is shown that all apecimens except one(No. 15) fail in shear. In Fig. 16, Q_{all} is compared with the maximum and minimum strengths, $\tilde{Q}_{max}$ and $\tilde{Q}_{min}$, of each specimen, where Q_{all} is the temporary allowable shear strength obtained from AIJ Standard published by Architectural Institute of Japan. In the figure, ${}_cQ$, ${}_rQ$ and ${}_sQ$ are contributions to Q_{all} from concrete, web reinforcement and steel web, and $Q_{Fc/15}$ is computed assuming that the maximum shear stress of concrete, τ is given by Fc/15(Fc: cylinder strength). The safety factor possessed by Q_{max} is about 1.4 in F series, and about 2.5 in L and B series, while the safety factor based on Q_{min} is less than 1.0 for some specimens in L and B series, although it is about 1.1 in F series. The effects of the experimental parameters, such as concrete strength, web thickness, lattice plate thickness, butten plate thickness, the amount of web reinforcement and the axial load are shown in Figs. 17(a) to (f), respectively. For the shear strength of the full-web type steel portion, ${}_{fs}Q_o$, the smaller value of the yield shear strength of the web, ${}_{fs}Q_{so}$, and ${}_{fs}Q_{mo}$ determined from the full plastic moment of the steel cross section, is taken. The smaller value of the shear strength based on the failure mechanism shown in Fig. 17(c)(or Fig. 17(d)), ${}_{ls}Q_{so}$(or ${}_{bs}Q_{so}$), and the shear strength based on the full plastic moment of the open-web steel cross section, ${}_{ls}Q_{mo}$ (or ${}_{bs}Q_{mo}$), it taken for the shear strength of the open-web steel portion, ${}_{ls}Q_o$(or ${}_{bs}Q_o$). From Fig. 17(a), it is observed that the shear strength obtained in the test increases with the increase of the concrete strength, and that the slope of the experimental curve is approximately equal to that of a straight line ${}_{c}Q_o= F_c \cdot b \cdot {}_{r}d/15$(b: width of concrete section, ${}_{r}d$: distance between upper and lower main reinforcing bars). It seems from Figs. 17(b), (c) and (d) that the rates of increase of the shear strength is approximately equal to those of ${}_{fs}Q_o$, ${}_{ls}Q_o$ and ${}_{bs}Q_o$, respectively, all of which are computed neglecting the bond action between steel and concrete. A similar statement seems to be also adequate for the effect of the web reinforcement, ${}_{r}P_w \cdot {}_{rw}\sigma_y \cdot b \cdot {}_{r}d$, in Fig. 17(e), where ${}_{r}P_w$ is the web reinforcement ratio, and ${}_{rw}\sigma_y$ yield stress of the web reinforcing bar. On the other hand the axial load does not affect on the shear strength, as seen in Fig. 17(f). Since the maximum shear strength is determined by the shear bond failure in the present test series, the result is different from the previously reported one that the axial load affects on the shear strength of the specimen failing in the diagonal tension.

5. CONCLUSIVE REMARKS

As already indicated, the shear bond failure plays a key role to determine the behavior of the steel reinforced concrete column under the axial load and alternately repeated shear. It is urgently needed to carry out the theoretical analysis associated with the development of the adequate mathematical model which explains the failure mechanism observed in the test.

REFERENCES

1. Tsuboi, Y. and Wakabayashi, M.:STUDY ON STEEL REINFORCED CONCRETE STRUCTURES, PART 5 - TESTS ON COLUMNS SUBJECTED TO AXIAL FORCE AND SHEAR, Trans. Architectural Institute of Japan, No. 56, June 1957, p. 39(In Japanese).

2. Wakabayashi, M.:EXPERIMENTAL STUDY ON COMPOSITE STRUCTURE, Report of the Institute of Industrial Science, University of Tokyo, Vol. 6, No. 2, Serial No. 45, Dec. 1956(In Japanese).

3. Wakabayashi, M., Minami, K. and Nakamura, T.:EXPERIMENTAL STUDIES ON STEEL-REINFORCED CONCRETE COLUMNS UNDER CONSTANT AXIAL FORCE AND ALTERNATE REPEATED BENDING AND SHEAR, Annuals, Disaster Prevention Research Institute, Kyoto University, No. 15-B, April 1973, p. 69(In Japanese).

4. Hirosawa, M., Ozaki, M. and Wakabayashi, M.:EXPERIMENTAL STUDY ON LARGE MODELS OF REINFORCED CONCRETE COLUMNS, Preprint of 5WCEE, Rome, June 25-29, 1973, No. 96.

ACKNOWLEDGEMENT

Research work presented here was supported by The Kozai Club and Building Research Institute, Ministry of Construction, Japan. Test apparatus was designed in Building Research Institute, and test was separately conducted in the laboratories of the following steel makers; Kawasaki Steel Corporation, Kobe Steel Ltd., Nippon Kokan K.K., Nippon Steel Corporation, and Sumitomo Metal Industry Ltd. Authors wish to express sincere appreciations for their supports.

TABLES AND FIGURES

Table 1. Test Program for Series F.

No.	Specimen Name	tf (mm)	tw (mm)	n	ϕ (mm)	s (mm)	Fc (kg/cm²)	N/No
1	12F8 M1216 W100 C210 N1	12	8	12	16	100	210	0.1
2	12F8 M1216 W100 C210 N2	12	8	12	16	100	210	0.2
3	12F8 M1216 W100 C210 N3	12	8	12	16	100	210	0.3
4	12F8 M1216 W100 C210 N1 *	12	8	12	16	100	210	0.1
5	12F8 M1216 W100 C210 N2 *	12	8	12	16	100	210	0.2
6	12F8 M1216 W100 C210 N3 *	12	8	12	16	100	210	0.3
7	12F6 M1216 W100 C210 N2	12	6	12	16	100	210	0.2
8	12F10 M1216 W100 C210 N2	12	10	12	16	100	210	0.2
9	8F6 M1216 W100 C210 N2	8	6	12	16	100	210	0.2
10	8F8 M1216 W100 C210 N2	8	8	12	16	100	210	0.2
11	8F10 M1216 W100 C210 N2	8	10	12	16	100	210	0.2
12	16F6 M1213 W100 C210 N2	16	6	12	13	100	210	0.2
13	16F8 M1213 W100 C210 N2	16	8	12	13	100	210	0.2
14	16F10 M1213 W100 C210 N2	16	10	12	13	100	210	0.2
15	12F8 M0413 W100 C210 N2	12	8	4	13	100	210	0.2
16	12F8 M1216 W150 C210 N2	12	8	12	16	150	210	0.2
17	12F8 M1216 W050 C210 N2	12	8	12	16	50	210	0.2
18	12F8 M1216 W025 C210 N2	12	8	12	16	25	210	0.2
19	12F8 M1216 W100 C250 N2	12	8	12	16	100	250	0.2
20	12F8 M1216 W100 C300 N2	12	8	12	16	100	300	0.2
21	12F8 M1216 W100 C350 N2	12	8	12	16	100	350	0.2

Table 2. Test Program for Series L.

No.	Specimen Name	θ (deg.)	tl (mm)	n	ϕ (mm)	s (mm)	Fc (kg/cm²)	N/No
22	45L8 M1216 W100 C210 N1	45	8	12	16	100	210	0.1
23	45L8 M1216 W100 C210 N2	45	8	12	16	100	210	0.2
24	45L8 M1216 W100 C210 N3	45	8	12	16	100	210	0.3
25	30L8 M1216 W100 C210 N1	30	8	12	16	100	210	0.1
26	30L8 M1216 W100 C210 N2	30	8	12	16	100	210	0.2
27	30L8 M1216 W100 C210 N3	30	8	12	16	100	210	0.3
28	45L6 M1216 W100 C210 N2	45	6	12	16	100	210	0.2
29	45L10 M1216 W100 C210 N2	45	10	12	16	100	210	0.2
30	45L8 M1216 W150 C210 N2	45	8	12	16	150	210	0.2
31	45L8 M1216 W050 C210 N2	45	8	12	16	50	210	0.2
32	45L8 M1216 W025 C210 N2	45	8	12	16	25	210	0.2

Table 3. Test Program for Series B.

No.	Specimen Name	p	tb (mm)	n	ϕ (mm)	s (mm)	Fc (kg/cm²)	N/No
33	75B8 M1216 W100 C210 N1	0.75	8	12	16	100	210	0.1
34	75B8 M1216 W100 C210 N2	0.75	8	12	16	100	210	0.2
35	75B8 M1216 W100 C210 N3	0.75	8	12	16	100	210	0.3
36	75B6 M1216 W100 C210 N2	0.75	6	12	16	100	210	0.2
37	75B10 M1216 W100 C210 N2	0.75	10	12	16	100	210	0.2
38	75B8 M1216 W150 C210 N2	0.75	8	12	16	150	210	0.2
39	75B8 M1216 W050 C210 N2	0.75	8	12	16	50	210	0.2
40	75B8 M1216 W025 C210 N2	0.75	8	12	16	25	210	0.2
41	90B8 M1216 W100 C210 N2	0.90	8	12	16	100	210	0.2
42	50B8 M1216 W100 C210 N2	0.50	8	12	16	100	210	0.2
43	M1816 W100 C210 N2			18	16	100	210	0.2

tf : Flange Thickness of Wide Flange Section
tw : Web Thickness of Wide Flange Section
tl : Lattice Plate Thickness
tb : Butten Plate Thickness
n : Number of Longitudinal Reinforcement
ϕ : Nominal Diameter of Longitudinal Reinforcement
s : Spacing of Web Reinforcement
Fc : Concrete Strength
N/No : Ratio of Axial Force to Ultimate Compressive Strength
θ : Angle of Inclination of Lattice Plate
p : Ratio of Spacing of Butten Plate to Depth of Steel Cross Section

* h/D = 5.

All dimensions shown in these tables are nominal.

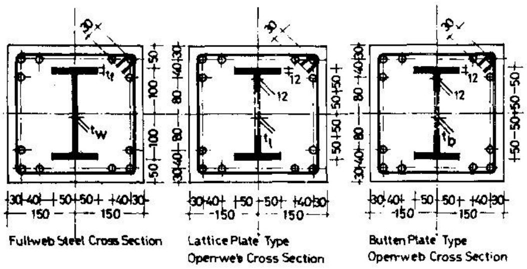

Fig. 1 Typical Column Cross Sections

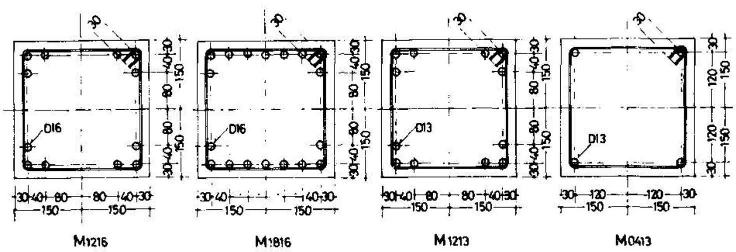

Fig. 2 Details of Reinforced Concrete Sections

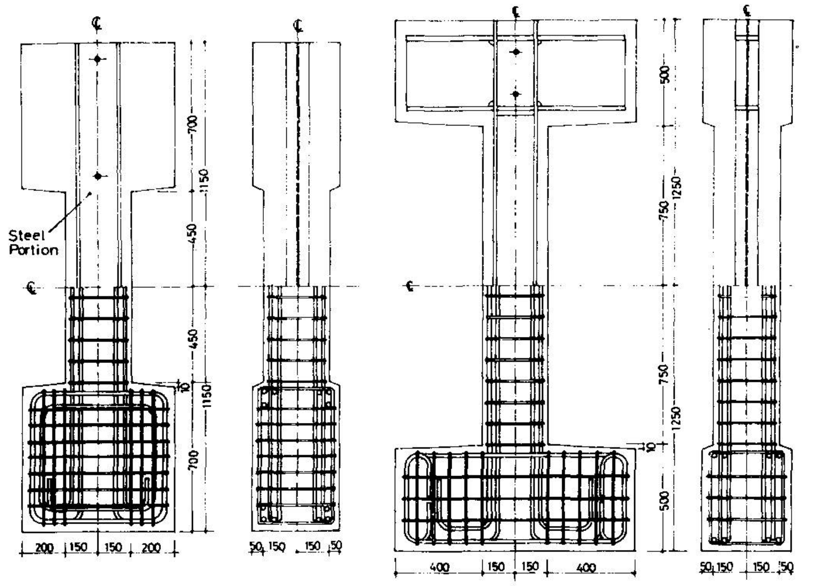

(a) h/D=3

(b) h/D=5

Fig. 3 Dimensions and arrangement of Reinforcements

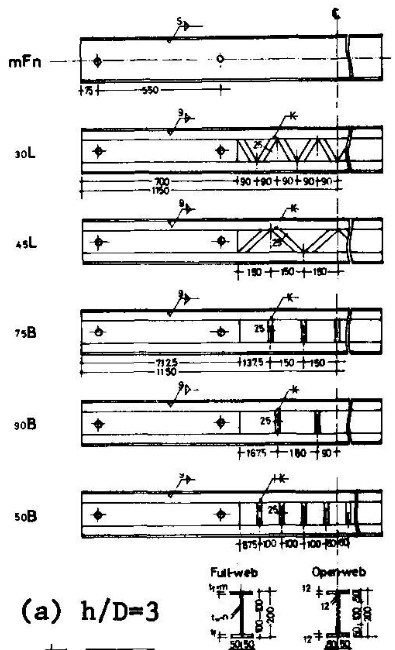

(a) h/D=3

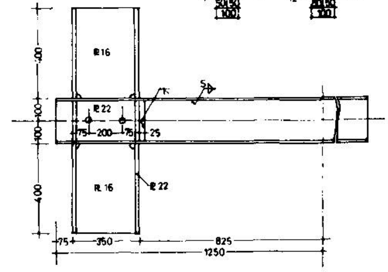

(b) h/D=5

Fig. 4 Dimensions of Steel portion

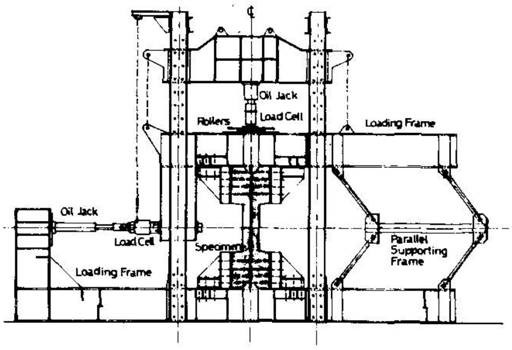

Fig. 5 Loading Apparatus

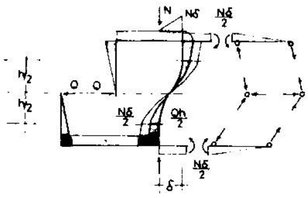

Fig. 6 Loading Principle

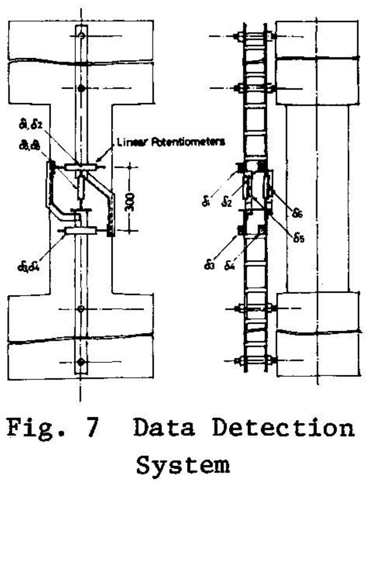

Fig. 7 Data Detection System

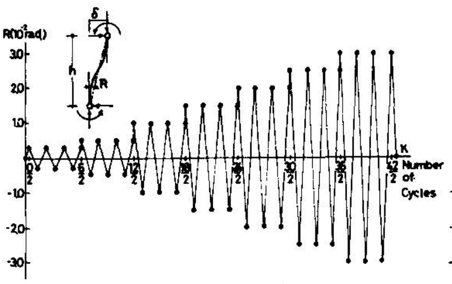

(a) h/D = 3

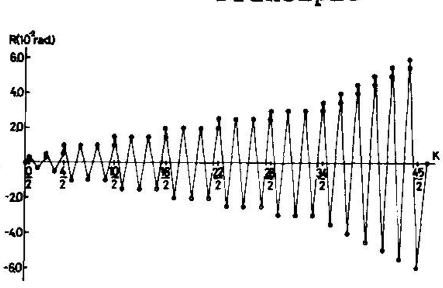

(b) h/D = 5

Fig. 8 Loading Program

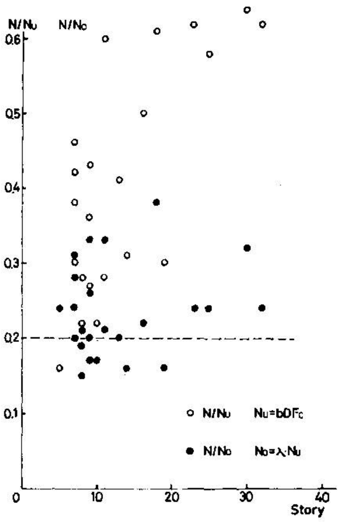

Fig. 9 Axial Loads in Columns

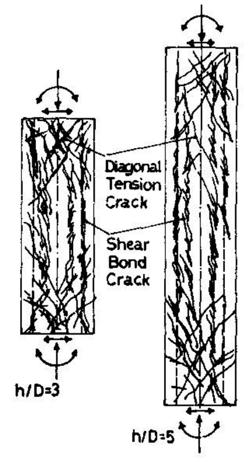

Fig. 10 Crack Observation

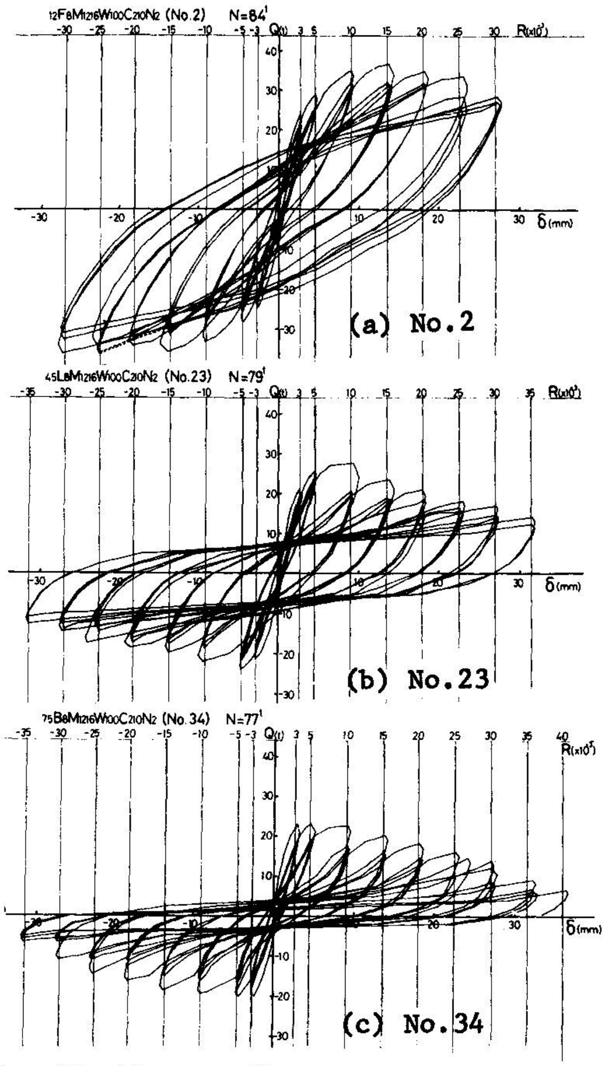

Fig. 11 Shear-Deflection Relationship

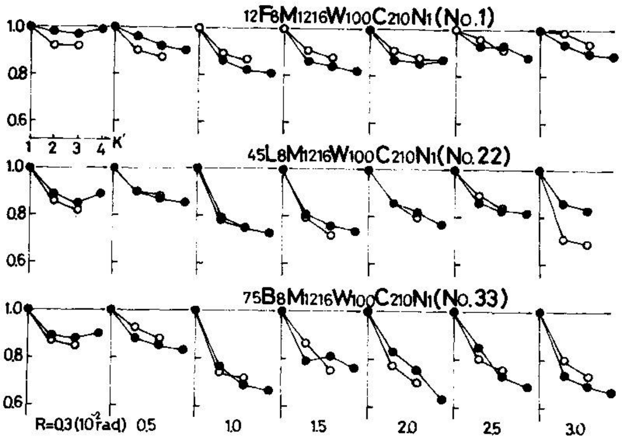

Fig. 12 Deterioration of Shear Strength

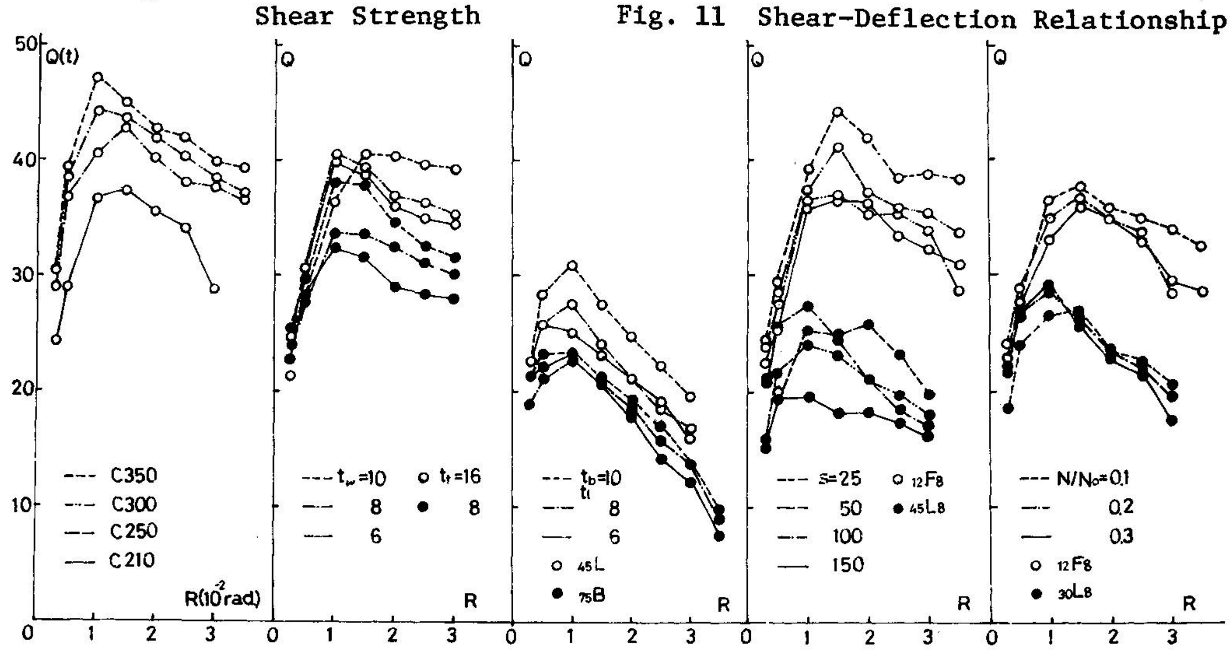

(a) Concrete Strength (b) Flange and Web Thickness (c) Lattice and Butten Plate Thickness (d) Spacing of Web Reinforcement (e) Axial Load Ratio

Fig. 12 Deterioration of Shear Strength

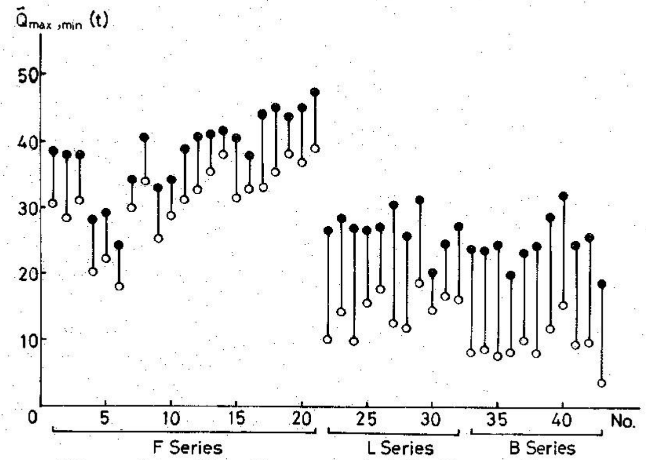

Fig. 14 Maximum and Minimum Shear

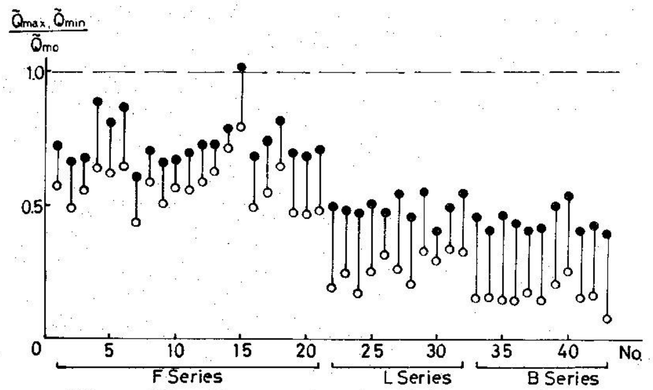

Fig. 15 Comparison of Strength

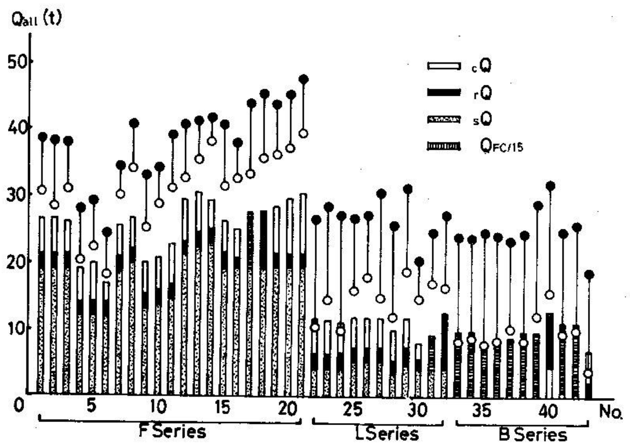

Fig. 16 Comparison of Measured and Allowable Shear Strength

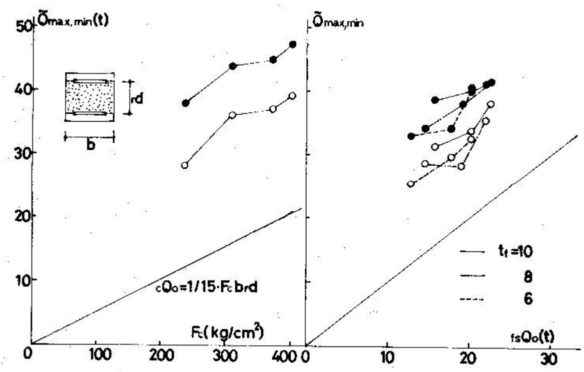

(a) Concrete Strength (b) Flange and Web Thickness

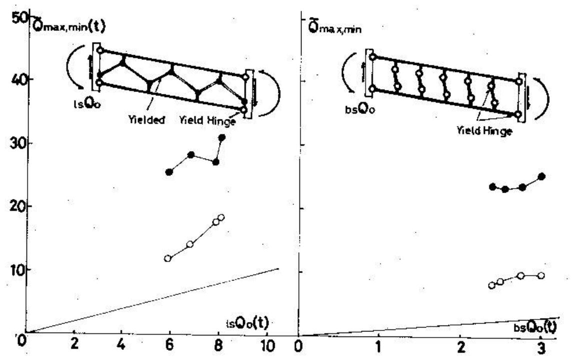

(c) Lattice Plate Thickness (d) Butten Plate Thickness

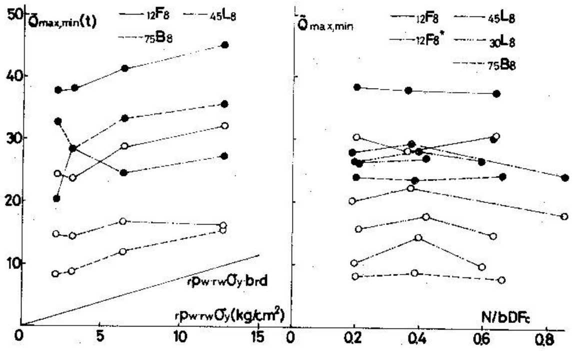

(e) Amount of Web Reinforcements (f) Axial Load

Fig. 17 Effects of Experimental Parameters

SUMMARY

A parametric experimental study is carried out on the shear strength of steel reinforced concrete (SRC) columns under constant axial load and alternately repeated bending and shear, using three types of steel sections; full-web type, lattice plate type open-web and butten plate type open-web. The effects of experimental parameters, such as axial load ratio, web plate thickness, spacing of web reinforcements, thickness of lattice and butten plates and concrete strength, on the shear strength and the hysteretic behavior of columns are discussed.

RESUME

On procède à une étude expérimentale de la résistance au cisaillement de colonnes en béton armé soumises à une force axiale constante et à une flexion et un cisaillement alternés; on utilise trois types de section pour l'armature. On discute l'influence des paramètres des essais, tels que grandeur de la force axiale, forme de l'armature et résistance du béton, sur la résistance au cisaillement et le comportement hystérétique des colonnes.

ZUSAMMENFASSUNG

Es wird eine experimentelle Untersuchung über den Einfluss verschiedener Parameter auf die Schubfestikeit von Stahlbetonstützen unter konstanter Normalkraft und abwechselnd wiederholter Beanspruchung auf Biegung und Schub durchgeführt. Hierbei werden drei Typen von Bewehrungs-Querschnitten untersucht. Die Wirkung des Versuchs-Parameter, wie z.B. die Grösse der Normalkraft, die Form der Bewehrung sowie die Betonfestigkeit auf die Schubfestigkeit und das Energieaufnahmevermögen der Stützen werden diskutiert.

Leere Seite
Blank page
Page vide